1   **Brown Adipose Tissue is Associated with Improved Cardiometabolic Health**

2   **and Regulates Blood Pressure**

3

4   Tobias Becher[1,9,10], Srikanth Palanisamy[1,2], Daniel J. Kramer[1,2,3], Sarah J. Marx[1], Andreas G.

5   Wibmer[4], Ilaria Del Gaudio[5,11], Scott D. Butler[6], Caroline S. Jiang[7], Roger Vaughan[2,7], Heiko

6   Schöder[4], Annarita Di Lorenzo[5], Allyn Mark[8] and Paul Cohen[1*]

7

8

9   [1]   Laboratory of Molecular Metabolism, The Rockefeller University, New York, NY

10   [2]   Weill Cornell Medicine, New York, NY

11   [3]   Weill Cornell/ Rockefeller/ Sloan Kettering Tri-Institutional MD-PhD Program, New York,

12   NY

13   [4]   Department of Radiology, Memorial Sloan Kettering Cancer Center, New York, NY

14   [5]   Department of Pathology and Laboratory Medicine, Cardiovascular Research Institute

15   and Feil Brain and Mind research Institute, Weill Cornell Medicine, New York, NY

16   [6]   Department of Biomedical Sciences, College of Veterinary Medicine, Cornell University,

17   Ithaca, NY

18   [7]   Center for Clinical and Translational Science, The Rockefeller University, New York

19   [8]   Department of Internal Medicine, Carver College of Medicine, University of Iowa, Iowa

20   City, Iowa

21   [9]   DZHK (German Centre for Cardiovascular Research), Partner Site

22   Heidelberg/Mannheim, Mannheim, Germany

23   [10]   First Department of Medicine (Division of Cardiology), University Medical Center

24   Mannheim, Mannheim, Germany

25   [11]   Department of Obstetrics and Gynecology, Medical University of Graz, Graz, Austria

26

27   **Corresponding Author:**

28   Paul Cohen, M.D., Ph.D.

29   E-Mail: pcohen@rockefeller.edu

30   The Rockefeller University

31   Laboratory of Molecular Metabolism

32   1230 York Avenue, P.O. Box 223, New York, NY 10065

33

34   **Abstract**

35   White fat stores excess energy, while brown and beige fat dissipate energy as heat[1]. These

36   thermogenic adipose tissues markedly improve glucose and lipid homeostasis in mouse

37   models, though the extent to which brown adipose tissue (BAT) influences metabolic and

38   cardiovascular disease in humans is unclear[2,3,4]. Here, we categorized 139,224 ^{18}F-FDG

39   PET/CT scans from 53,475 patients by presence or absence of BAT and used propensity score

40   matching to assemble a study cohort. Individuals with BAT showed lower prevalences of

41   cardiometabolic diseases. Additionally, BAT independently correlated with lower odds of type II

42   diabetes, coronary artery disease and congestive heart failure. These findings were supported

43   by improved glucose, triglyceride and high-density lipoprotein values. The effects of BAT were

44   more pronounced in overweight and obesity, indicating that BAT can offset the deleterious

45   effects of obesity. Strikingly, we also found lower rates of hypertension among patients with

46   BAT. Studies in a mouse model with genetic ablation of beige fat demonstrated elevated blood

47   pressure due to increased sensitivity to angiotensin II in peripheral resistance arteries. In

48   addition to highlighting a role for BAT in promoting overall cardiometabolic health, this study

49   reveals a new link between thermogenic adipose tissue and blood pressure regulation.

3

50   **Main**

51   As early as 2003, reports described increased uptake of the labeled glucose analogue

52   ^{18}F-fluorodeoxyglucose (^{18}F-FDG) on positron emission tomography (PET) in areas

53   corresponding to supraclavicular fat on computed tomography (CT), suggesting the presence of

54   metabolically-active BAT in adult humans[5,6]. This tissue has received intense interest from the

55   biomedical community since 2009 when a series of papers confirmed the presence of active

56   BAT in adults, which correlated with lower body mass index (BMI), decreased age, colder

57   outdoor temperature, and female sex, as well as an association with decreased fasting glucose

58   levels[7,8,9,10,11,12]. Since then, small prospective studies in healthy humans have demonstrated

59   that cold-activated BAT is associated with increased whole body energy expenditure and

60   increased disposal of glucose and free fatty acids[13,14,15]. Although these properties have

61   generated great enthusiasm for BAT as a therapeutic target for obesity and its associated

62   diseases, these studies have been too small to definitively address whether brown fat is a

63   clinically meaningful modulator of metabolic and cardiovascular disease in humans.

64   To answer this central question, we reviewed 139,224 ^{18}F-FDG PET/CT reports

65   conducted in 53,475 patients between June 2009 and March 2018 at Memorial Sloan Kettering

66   Cancer Center (MSKCC) (**Fig. 1a**). ^{18}F-FDG PET/CT was conducted for cancer diagnosis,

67   staging, monitoring of treatment response, and surveillance, and it is protocol at MSKCC to

68   report on BAT status in each study. BAT was reported on 7,923 (5.7%) ^{18}F-FDG PET/CT scans

69   (**Fig. 1b, Extended Data Table 1**) in 5,070 (9.5%) patients (**Fig. 1c, Extended Data Table 2**),

70   consistent with prior studies[5,6,11,16]. To assess accuracy of reporting and our search strategy, all

71   scans conducted in 2016 with reported BAT were manually reviewed. Of the 1,139 scans that

72   reported brown fat in 2016, 1,132 (99.4%) PET scans showed increased ^{18}F-FDG uptake in

73   regions identified as fat on CT in typical locations (neck, supraclavicular, axillary, mediastinal,

74   paraspinal and abdominal) while 4 (0.4%) scans reported a possible signature and 3 (0.3%)

75   scans were false-positive since they reported resolution of previously reported brown fat. While

76   the usage of ^{18}F-FDG PET/CT increased over the years in this study, the prevalence of BAT

77   reporting remained consistent (**Extended Data Fig. 1**).

78   Patients were categorized by the presence or absence of BAT, and for those with

79   multiple scans an index scan was assigned (**Fig. 1a**, described in methods). Brown fat was

80   more prevalent among women (13.6 vs. 4.8%, *P*<0.0001), decreased with age (r=-0.9842,

81   *P*<0.0001), and was inversely correlated with ambient temperature (r=-0.7093, *P*<0.0001) and

82   BMI (r=-0.4360, *P*=0.0007), in accord with prior smaller retrospective studies (**Fig. 1d-g and**

83   **Extended Data Fig. 2a and b**)[10,11].

84   Propensity score matching (PSM) allows for pairing of subjects with and without brown

85   fat, while accounting for covariates that predict the likelihood of having brown fat. We used PSM

86   to generate a study cohort without brown fat (*N* = 5,070), matching the individuals with brown fat

87   based on sex, age, BMI and outdoor temperature at the time of the index scan (**Fig. 1h**). This

88   resulting study cohort was balanced across the aforementioned variables (**Tab. 1; Extended**

89   **Data Fig. 3**).

90   Individuals with brown fat showed significantly lower prevalence of type II diabetes (4.6

91   vs. 9.1%, *P*<0.0001) and dyslipidemia (18.9 vs. 20.6%, *P*=0.0318). This protective effect was

92   also seen for cardiovascular disease, including atrial fibrillation/flutter (2.8 vs. 3.7%, *P*=0.0071),

93   coronary artery disease (3.1 vs. 5.0%, *P*<0.0001), cerebrovascular disease (2.1 vs. 3.1%,

94   *P*=0.0011), congestive heart failure (1.0 vs. 2.1%, *P*<0.0001) and hypertension (26.7 vs. 29.6%,

95   *P*=0.0003) (**Fig. 2a**).

96   Cancer-associated characteristics such as cachexia, cancer type and stage have

97   previously been associated with differences in brown fat prevalence on ^{18}F-FDG PET/CT, as

98   has the use of beta-blocker drugs[11,17,18,19]. These associations were also observed in our study

99   (**Extended Data Table 3 and Table 1**). We used logistic regression analysis, adjusted for

100   cancer site, cancer stage, and beta-blocker use, and demographic variables (including race,

101   ethnicity, smoking status) to determine whether brown fat independently correlated with

5

102 cardiometabolic disease. Multivariable logistic regression analysis identified brown fat as an

103 independent negative predictor of type II diabetes (OR=0.46; 95% CI=0.39-0.55; *P*<0.0001),

104 coronary artery disease (OR=0.63; 95% CI=0.50-0.79; *P*<0.0001), congestive heart failure

105 (OR=0.56; 95% CI=0.40-0.80; *P*=0.0012) and hypertension (OR= 0.88; 95% CI=0.79-0.97;

106 *P*=0.0130) (**Fig. 2b and Extended Data Table 4**).

107   Next, we stratified these data by BMI to determine whether the association between

108 brown fat and improved cardiometabolic health was retained in overweight and obese

109 individuals. As the prevalence of metabolic and cardiovascular disease increased with higher

110 BMI, this effect was mitigated in individuals with brown fat (**Fig. 2c**). The benefit associated with

111 brown fat was most striking for type II diabetes and coronary artery disease. For example, the

112 prevalence of type II diabetes in individuals with BMI > 30 kg/m^2 and brown fat was less than

113 half of the prevalence in obese individuals without brown fat (7.5 vs. 19.1%, *P*<0.0001).

114 Significantly lower prevalences of hypertension (39.9 vs. 47.0%, *P*=0.0020) and congestive

115 heart failure (1.1 vs. 2.9%, *P*=0.0060) were also observed in individuals with obesity and brown

116 fat. Using the multivariable logistic regression model described above, we confirmed that brown

117 fat was independently associated with the observed decrease in cardiometabolic disease

118 prevalence in obese individuals (**Fig 2c**).

119   Next, we analyzed available laboratory values in temporal vicinity to the index scan to

120 further characterize the metabolic profile of the cohort. We noted distinct improvements in

121 glucose (91.7 vs. 95.1 mg/dl, *P*<0.0001), triglycerides (122.4 vs. 148.4 mg/dl, *P*=0.0006), and

122 HDL levels (56.4 vs. 52.2 mg/dl, *P*=0.0001) in individuals with brown fat, while there were no

123 differences for LDL (112.1 vs. 110.3 mg/dl, *P*=0.4406) and total cholesterol (192.3 vs. 188.6

124 mg/dl, *P*=0.1492) (**Fig. 2d and Extended Data Table 5**). By stratifying laboratory values by

125 BMI, we found that changes in fasting blood glucose and triglycerides associated with elevated

126 BMI were offset in individuals with brown fat, and HDL levels were higher across all BMI

127 categories in individuals with brown fat (**Fig. 2d**). There were no apparent differences in

6

128   laboratory values measuring renal function (creatinine 0.83 vs. 0.84 mg/dl, P=0.4537 and blood

129   urea nitrogen 14.6 vs. 14.8 mg/dl, P=0.1532) and thyroid function (TSH 2.95 vs. 2.49 mIU/L,

130   P=0.1764) (**Extended Data Table 5**). However, both leukocyte (6.2 vs. 6.8 10^9 cells/L,

131   P<0.0001) and platelet counts (250 vs. 260 10^9 cells/L, P=0.0007) were significantly decreased

132   in subjects with brown fat, suggesting potential roles for brown adipose beyond direct regulation

133   of lipid and glucose metabolism (**Extended Data Table 5**). In summary, our data support an

134   important role for brown fat in mitigating metabolic disease and its cardiovascular sequelae,

135   particularly in obese individuals.

136   Thermogenic fat promotes energy expenditure, and there is increasing evidence that this

137   tissue plays roles in metabolism beyond thermogenesis itself[20,21,22]. While thermogenesis clearly

138   modulates glucose and lipid metabolism, an association between thermogenic fat and blood

139   pressure has not been described until now. Furthermore, transcriptomic profiling indicates that

140   murine beige fat, as opposed to developmentally pre-formed brown fat, closely approximates

141   the inducible brown fat detected by PET/CT in adult humans[23]. We therefore used adipocyte-

142   specific PRDM16 knockout (Adipo-PRDM16 KO) mice (**Extended Data Fig. 4a, b, and c**) with

143   an ablation of beige fat function to investigate the potential link between thermogenic fat and

144   blood pressure control[24]. Interestingly, a previous genome-wide association study demonstrated

145   an association between a coding SNP in exon 9 of PRDM16 (leading to the missense mutation

146   Pro633Leu) and hypertension in humans[25].

147   Adipo-PRDM16 KO animals were implanted with radiotelemetric devices to monitor

148   blood pressure over a three-week period (**Fig. 3a**). Our studies were conducted in 11 to 14-

149   week-old mice on a standard chow diet, and body weight was equivalent between genotypes

150   throughout the study (**Extended Data Fig. 4d**). Significant increases in systolic (difference

151   between means 3.6 mmHg; 95% CI 0.9-6.4, P=0.0102), diastolic (difference between means

152   4.2 mmHg; 95% CI 1.2-7.2, P=0.0071), mean arterial blood pressure (difference between

153   means 4.0 mmHg; 95% CI 1.8–6.3, P=0.0007) and heart rate (difference between means 18

154   bpm, 95% CI 3-33, *P*=0.0202) were apparent in KO animals versus controls (**Fig. 3a and**

155   **Extended Data Table 6**). After adjustment for heart rate, genotype remained independently

156   associated with increased systolic (difference between means 2.8 mmHg; 95% CI 0.2–5.5,

157   *P*=0.0378), diastolic (difference between means 3.3 mmHg; 95% CI 0.4–6.2, *P*=0.0281) and

158   mean arterial blood pressure (difference between means 3.3 mmHg; 95% CI 1.0–5.6,

159   P=0.0052) (**Extended Data Table. 7**).

160   There were no significant differences in heart weight, wall thickness, cardiac function or cardiac

161   tissue histology, indicating that neither cardiac morphology nor function were responsible for the

162   observed differences in systemic blood pressure (**Fig. 3b and Extended Data Fig. 5a**). We thus

163   explored resistance vasculature morphology and function. By using the pressure myograph

164   system, second order mesenteric arteries isolated from Adipo-PRDM16 KO mice (after

165   dissecting off all perivascular fat) demonstrated an increased contractile response specifically to

166   angiotensin II, with no significant differences in response to acetylcholine or phenylephrine (**Fig.**

167   **3c**). Additionally, vasodilation in response to a stepwise increase in flow was significantly

168   decreased in Adipo-PRDM16 KO mice while myogenic tone induced by a stepwise increase in

169   pressure did not show a difference between the genotypes (**Extended Data Fig. 5b)**.

170   Histological analysis evidenced no apparent structural differences (**Fig. 3d**). There were no

171   significant differences in plasma levels of angiotensinogen (**Fig. 3e**) or expression of

172   angiotensin receptors in the mesenteric arteries (**Fig. 3f**). In summary, ablation of beige fat

173   function in mice leads to an increased sensitivity of resistance arteries to angiotensin II,

174   contributing to elevated systemic blood pressure.

175   Obesity is a major contributor to metabolic and cardiovascular disease, and 48.9% of

176   American adults are predicted to be obese by 2030[26]. With limited effective therapies available,

177   thermogenic fat has been implicated as a potential therapeutic target for obesity and metabolic

178   disease[27]. In healthy adults, cold stimulation of brown fat increases energy expenditure and

179   improves systemic glucose utilization, fatty acid oxidation, and insulin sensitivity[28,29,30,31]. This

180   observation is consistent with animal models, where transplantation of thermogenic adipose

181   tissue mass improved glucose and triglyceride metabolism, while genetic ablation of

182   thermogenic fat had the opposite effect[3,32,33]. The effects of thermogenic adipose tissue on

183   cardiometabolic health and obesity-associated diseases in humans, however, have been largely

184   unexplored until now.

185   Our study illustrates that individuals with thermogenic fat on ^{18}F-FDG PET/CT have

186   significantly improved metabolic profiles. This effect is not only limited to diabetes, but extends

187   to coronary artery disease, congestive heart failure and hypertension. Furthermore, the effects

188   of brown fat on metabolic and cardiovascular disease are most pronounced among individuals

189   with elevated BMI. While obesity is generally associated with decreased brown fat function[34],

190   those obese individuals who retain brown fat activity appear to be protected against conditions

191   linked to excess weight. This notion further supports the potential of brown fat as a therapeutic

192   target beyond weight loss itself, but as a means to uncouple obesity from disease.

193   The reduction in the prevalence of hypertension associated with thermogenic fat was of

194   particular interest to us, because this cannot be directly explained by improvements in glucose

195   and lipid metabolism. Our studies in a mouse model lacking beige fat identified changes in

196   sensitivity to angiotensin II in the peripheral resistance vasculature as a potential underlying

197   physiological mechanism. Thermogenic fat secretes a number of endocrine factors that can

198   affect a wide variety of tissues, and ongoing research is focused on elucidating the downstream

199   effectors of these signals. Our work points towards a novel molecular signal linking adipose

200 tissue phenotype to blood pressure control, and may be the first step in elucidating a

201 mechanistic link between brown fat and hypertension.

202 Our study raises a number of questions regarding brown fat development and function in

203 humans. Variability in brown fat prevalence and activity suggests a possible genetic determinant

204 of its biology. Consistent with this, our understanding of genetics as a contributor to type II

205 diabetes development has evolved significantly[35]. It is likely then that genetic factors

206 contributing to brown fat development and activity may affect the pathogenesis of type II

207 diabetes and metabolic syndrome. In our study, brown fat was associated with improved health

208 across several organ systems. As an example, individuals without brown fat exhibited higher

209 leukocyte counts, and elevated white blood cell counts are an established risk factor for

210 coronary artery disease[36,37,38]. Decreased leukocyte counts in individuals with brown fat could, in

211 part, explain the lower prevalence of coronary artery disease among these subjects. Our work

212 highlights the need to determine the extent of brown fat's effects on other organs and roles in

213 systemic metabolism.

214 The major strength of our study is the size of the dataset, the largest we are aware of,

215 and the linkage to electronic health records. This allowed us to comprehensively examine

216 associations between brown fat and a wide variety of data. There are, however, a number of

217 limitations that need to be acknowledged, mainly pertaining to the retrospective design and

218 analysis of data from a cancer population. First, identification of brown fat relies on ^{18}F-FDG

219 PET/CT and consistent reporting. Our manual review of brown fat reporting over an entire year,

220 as well as a consistent brown fat prevalence over the study period, support the reliability of

221 reporting in this study. Furthermore, ^{18}F-FDG PET/CT without prior cold stimulation tends to

222 underestimate brown fat prevalence, which may have impacted our classification. In the

223 absence of broadly applicable screening methods or biomarkers for brown fat, the application of

224 ^{18}F-FDG PET/CT to screen for brown fat is however still considered the gold standard. Although

225 a number of studies have indicated associations between cancer characteristics and brown fat

226　　prevalence as measured by ^{18}F-FDG PET/CT, the effect of cancer is still poorly understood. We

227　　have thus adjusted our analysis to accommodate the potential influence of cancer type and

228　　stage.

229　　　　In our study, we investigated and confirmed new clinical findings linking thermogenic

230　　adipose tissue and improvements in metabolic health using an established mouse model. These

231　　findings will have the potential to enable translation of animal findings into viable human

232　　therapies. Our study highlights the therapeutic potential of modulating brown fat in humans to

233　　combat the escalating obesity crisis.

234

235 **Online Methods**

236 **Study Design and Participants**

237 This retrospective case-control study followed institutional guidelines and was approved by the

238 Institutional Review Boards of The Rockefeller University and Memorial Sloan Kettering Cancer

239 Center (MSKCC). Due to the retrospective nature of this study, the requirement for informed

240 consent was waived. Results from this study are reported in accordance with the Strengthening

241 the Reporting of Observational Studies in Epidemiology (STROBE) guidelines for case-control

242 studies[39].

243 We identified all patients age 18 and above who underwent ^{18}F-FDG PET/CT at MSKCC from

244 June 2009 through March 2018. This resulted in 139,224 ^{18}F-FDG PET/CT scans conducted in

245 53,475 patients. Brown adipose is identified by increased ^{18}F-FDG uptake on PET, measured in

246 regions corresponding to adipose tissue on CT, and it is standard practice at MSKCC to

247 document these signatures in all reports. We searched all ^{18}F-FDG PET/CT reports for the

248 terms "brown fat" or "brown adipose". Patients were then categorized by the presence or

249 absence of brown fat reporting. For each subject in both groups, an index scan was designated

250 as follows: in patients with brown adipose tissue reported on at least one ^{18}F-FDG PET/CT

251 scan, the first scan that reported brown fat was defined as the index scan. In patients without

252 brown fat on any scan, the first ^{18}F-FDG PET/CT scan served as the index scan (**Fig. 1**).

253

254 **Data collection**

255 We obtained average outdoor temperatures in New York City, measured in Central Park, for the

256 months of scans from the U.S. National Weather Service. All patient data including

257 demographics and self-reported race and ethnicity were collected from institutional electronic

258 health records (EHR). Diagnoses listed up to one year after the time (month and year) of the

259 index scan were identified using diagnostic codes from the International Classification of

260 Diseases, 9th and 10th Revisions (ICD-9 and ICD-10) (**Supplementary Data Table 1**).

261   Laboratory values were recorded from the EHR if these values were first measured within three

262   months (complete blood counts) or one year (lipid levels) of the index scan date. In case of

263   multiple data points available, the one closest to the index scan was used for analysis. Blood

264   glucose was routinely measured on the day of scanning. Complete blood counts from patients

265   with hematological malignancies were excluded from analysis. With the exception of fasting

266   blood glucose, measurement of blood values was not coupled to ^{18}F-FDG PET/CT scans. Data

267   completeness was assessed for all blood values, and available data was analyzed using

268   complete case analysis (**Extended Data Table 5**). Data completeness ranged from 11.7% (low-

269   density lipoproteins) to 98.1% (glucose).

270

271   **Propensity Score Matching and Identification of Study Cohort**

272   To identify the study cohort, patients with reported brown fat were matched to patients without

273   reported brown fat using propensity score matching. Propensity scores were estimated using a

274   non-parsimonious multivariable logistic-regression model with brown adipose tissue status

275   (presence or absence) as the dependent variable and age, sex, BMI, and temperature at time of

276   scan as covariates. Matching was performed using a 1:1 protocol without replacement (greedy-

277   matching algorithm), a caliper width of 0.2 and the variable sex was set to be exactly matched.

278   We used standardized difference means to assess balance before and after matching

279   (**Extended Data Fig. 3**). Matching was conducted in SAS version 9.4 (SAS Institute, Cary, NC)

280   using the **psmatch** function.

281

282   **Outcomes**

283   ICD-9/10 diagnoses extracted from EHRs were used to examine associations between brown

284   fat and cardiometabolic health defined as the prevalence of type II diabetes, dyslipidemia,

285   hypertension, coronary artery disease, congestive heart failure and cerebrovascular disease. All

286   ICD-9/10 codes used to assign disease categories are listed in **Supplementary Data Table 1**.

287

288 **Data Analysis**

289 We first assessed the correlation between brown fat and age, outdoor temperature in the month

290 of the ^{18}F-FDG PET/CT index scan and BMI. For age and BMI, a one-phase exponential decay

291 curve was modeled and the correlation was assessed by calculating Spearman's rank

292 correlation coefficient. For temperature, a linear regression line was calculated and the

293 correlation was assessed by calculating Spearman's rank correlation coefficient. Prevalence of

294 brown fat in men and women was compared using chi-squared test. Brown adipose status

295 (either present or absent) and prevalence of cardiometabolic diseases were compared using

296 chi-squared tests.

297 Next, we assessed whether brown fat status was an independent predictor of cardiovascular

298 disease by using multivariable logistic regression analysis. The dependent variable in this

299 analysis was the respective cardiometabolic disease and brown fat status (presence or

300 absence) was the independent variable. To adjust for potential confounders that were selected

301 based on previous publications, we controlled for the following variables: age, sex, BMI, outdoor

302 temperature in Central Park in the month of the index scan, smoking status, race, ethnicity,

303 family history of cardiovascular disease, beta blocker use, cancer site, and cancer stage.

304 Smoking was coded as a categorical variable with 4 levels (current smoker, previous smoker,

305 never smoker, unknown smoking status). Race was a categorical variable with 4 levels:

306 Caucasian, African-American, Asian and other (e.g. Pacific-Islanders, unknown). Ethnicity was a

307 categorical variable with three levels: Hispanic, Non-Hispanic and Unknown. Cancer stage was

308 a 6 level categorical variable consisting of Stages I-IV, not applicable (e.g. hematologic

309 malignancies, benign tumors), and unknown cancer stage. Cancer site was recorded according

310 to ICD 0 Site Codes and included 14 categories: C00-C14, C15-C26, C30-C39, C40-C41, C42,

14

311   C43-C44, C45-C49, C50-C58, C60-C63, C64-C68, C69-C72, C73-C75, C76-C80 and

312   other/unknown. Results were reported as odds ratio and 95% confidence interval.

313   Cardiometabolic diseases that were independently associated with brown fat status were further

314   stratified by BMI categories (normal weight, defined as BMI <25km/m^2; overweight, defined as

315   BMI $25.0 - 30.0$ kg/m^2; obese, defined as BMI >30.0 kg/m^2). Comparison between individuals

316   with and without brown fat in the respective category were performed using the multivariable

317   logistic expression model outlined above to assess whether observed differences were

318   statistically significant. For the comparison of laboratory values, a Student's t-test was

319   performed. To compare associations between brown fat status, BMI and available lab values, a

320   least squares linear regression line was constructed, stratified by brown status. All p-values are

321   two-tailed, and values less than 0.05 were considered statistically significant.

322

Animal Experiments

324   Animal care and experimentation were performed according to procedures approved by the

325   Institutional Animal Care and Use Committee at the Rockefeller University. The Adipo-PRDM16

326   KO mice were generated by breeding Prdm16lox/lox mice with Adiponectin-cre mice (provided

327   by Dr. Evan Rosen, backcrossed to a C57BL/6J background)[24]. Mice were maintained in 12 hr

328   light:dark cycles at 23C and fed a standard irradiated rodent chow diet.

329

RNA Preparation and Quantitative PCR

331   Total RNA was extracted from adipose tissue using TRIzol (Cat # 15596018, Thermo Fisher

332   Scientific, Waltham, MA, USA) along with RNeasy mini kits (Cat # 74104, QIAGEN, Venlo,

333   Netherlands). For qPCR analysis, RNA was reverse transcribed using the ABI high capacity

334   cDNA synthesis kit (Cat # 4368813, Thermo Fisher Scientific, Waltham, MA, USA). cDNA was

335   used in qPCR reactions containing SYBR-green fluorescent dye (Cat # 4309155, Thermo Fisher

336   Scientific, Waltham, MA, USA). Relative mRNA expression was determined by normalization

15

337   with Eukaryotic 18S ribosomal RNA levels using the DDCt method. Primer sequences are listed

338   in **Supplementary Data Table 2.**

339

340   **Implantation of Radiotelemetry Devices and Blood Pressure Measurement**

341   Blood pressure was measured by implantable radio transmitters as previously described[40].

342   Briefly, male mice at age 11-14 weeks were housed in pairs. Prior to implantation, the animals

343   received buprenorphine (0.8 mg/Kg, s.c.) and a transmitter was implanted (model HD-X11, Data

344   Sciences International, St. Paul, MN, USA), while mice were under isoflurane anaesthesia. The

345   catheter tip was positioned in the thoracic aorta via the left common carotid artery and the body

346   of the probe was inserted subcutaneously in the dorsal right flank. Animals were allowed to

347   recover for 5–7 days. Heart rate (HR), systolic blood pressure (SBP), diastolic blood pressure

348   (DBP), and mean arterial pressure (MAP) were collected weekly over a 24h period in freely

349   moving conscious mice in their cages. Pressure traces were checked and animals with damping

350   of the haemodynamic profile were excluded from the analysis

351

352   **Analysis of Blood Pressure Readings**

353   For each mouse, systolic, diastolic and mean arterial blood pressure as well as heart rate was

354   recorded. The mean for each parameter was calculated over a 24h period. Data from 4

355   experiments were pooled and used for the final analysis. A linear mixed model for repeated

356   measures over time (SAS Proc Mixed) was used to analyze the radiotelemetry data with fixed

357   effects of genotype (KO vs. WT), week treated as a categorical factor, and the interaction

358   between genotype and week. This method prevented list-wise deletion due to missing data.

359   Unstructured covariance structure was chosen with the lowest corrected Akaike's

360   information criteria and Bayesian information criteria. Heart rate was included as a covariate for

361   the blood pressure models and the adjusted mean difference between KO and WT mice with 95

362   % confidence intervals were reported.

363

Mass Spectrometry

365 12 µl of serum sample were incubated with 12 µL of 20mM dithiothreitol (DTT) and 16 M urea

366 (final 8M urea, 10 mM DTT, 50mM ammonium bicarbonate (ABC)) for 1h at room temperature

367 (RT). Another 6 µL of 50mM DTT were added to the samples (in 50 mM ABC, no urea) to

368 ensure complete reduction. The samples were then alkylated by addition of 20 µL of 75mM

369 iodoacetamide (IAA; 30mM final in ABC) in the dark at RT for 1.5h. 6 µg of LysC was added to

370 each of the sample. The samples were then allowed to digest at 28° C overnight with shaking.

371 The following day, the samples were further diluted with 60 µL of 50mM ABC. 10 µg of trypsin

372 was added to each of the samples and samples were digested with trypsin for 6 hours at 28° C

373 at 1400 rpm. The samples were then quenched with 10 µL of 10% TFA (pH approximately 1). 5

374 µL of sample was loaded onto 4 C18 empore discs. The cleaned up samples were speed

375 vacuumed and re-dissolved in 20 µL of 0.1% LC-grade formic acid. 1 uL was loaded onto a

376 reverse-phase nano-LC-MS/MS (EasyLC 1200, Fusion Lumos, Thermo Fisher Scientific) for

377 analysis. Peptides were separated with a gradient in which the proportion of buffer B (H2O with

378 0.1% formic acid) in buffer A (acetonitrile with 0.1% formic acid) increased from 2% to 90% over

379 79 minutes (300 nl/min flow rate). MS and MS/MS data were recorded at resolutions of 60.000

380 and 30.000 with AGC's of 1,000,000 and 50,000 respectively. Parallel reaction monitoring

381 (PRM) was used to target peptides unique to AGT

382 (AIQGLLVTQGGSSSQTPLLQSIVVGLFTAPGFR and LPTLLGAEANLNNIGDTNPR). PRM

383 experiment data were analyzed with SkyLine v.4.2. Samples were analyzed in the following

384 order: KO, WT and values were normalized to WT to derive fold-change between the two

385 genotypes.

386

387

388

Tissue Staining

Mesenteric arteries and hearts were collected from 18-week-old male mice. Briefly, mice were euthanized by isoflurane overdose and the mesenteric artery was isolated and perfused with 50 mmol/L PBS (pH 7.4) followed by 4% PFA. After fixation overnight, tissues were washed 3x with PBS and stored in ethanol 70%. Further tissue processing was performed at the Memorial Sloan Kettering Cancer Center (MSKCC) Laboratory of Comparative Pathology. Briefly, the tissues were embedded in paraffin and the dewaxed slides were first immersed in Weigert's hematoxylin (Sigma, St. Louis, MO, U.S.A.), followed by serial staining with acid fuschin, phosphomolybdic acid and methyl blue. The tissues were then fixed in 1% acetic acid. After dehydration with increasing concentrations of alcohol, the slides were fixed in toluene, mounted in Permount and air-dried overnight before acquiring photographs.

Echocardiography

Mice were anaesthetized with isoflurane under continuous monitoring and placed on a heating pad of a recording stage connected to a Vevo 2100 ultrasound machine. The anterior chest wall was shaved, ultrasound gel was applied and electrodes were connected to each limb to simultaneously record an electrocardiogram. Two-dimensional (short axis-guided) M-mode and B-mode measurements (at the level of the papillary muscles) were taken using an 18–32 MHz MS400. For analysis, at least three measurements were averaged; measurements within the same HR interval (450 ± 50 bpm) were used for analysis.

Pressure myography

Mesenteric arteries were collected from 18-week-old male mice, as described above. Second order mesenteric arteries (MA) were cleaned of surrounding fat and vascular reactivity experiments were performed as described previously [41]. Briefly, MA were mounted on glass cannulas in a pressure myograph chamber (Danish MyoTechnology, Aarhus, Denmark) The

18

415   vessel orientation in relation to the flow *in vivo* was maintained. Vessel viability was maintained

416   using Krebs solution solution (in mM: NaCl 118, KCl 4.7, $MgCl_2$ 1.2, KH_2PO_4 1.2, $CaCl_2$ 2.5,

417    $NaHCO_3$ 25 and glucose 10.1), at 37 °C and oxygenated (95% O_2 and 5% CO_2). A pressure

418   interface controlled intraluminal pressure and flow in MA. The vessel diameter was monitored in

419   real time using a microscope connected to a digital video camera (IC Capture) and computer

420   software VediView 1.2 (Danish MyoTechnology, Aarhus, Denmark) with edge detection

421   capability. MA were equilibrated for 15 min at 80 mm Hg, pre-constricted with PE (1 µM) and a

422   cumulative concentration-response curve of Ach (0.1 nM – 30 µM) was performed to evaluate

423   the integrity and the function of the endothelium. MA with less than 80% vasodilatory response

424   to Ach were discarded. Vascular smooth muscle functions were evaluated by performing

425   cumulative concentration-response curves of PE (1 nM – 30 µM), AngII (0.1 nM – 1 µM) and

426   myogenic tone. Flow mediated vasodilation was also evaluated as previously described [41].

427

Statistical Analysis

429   Unless otherwise stated, data are presented as mean ± s.e.m. and are derived from multiple

430   experiments. Normality was assessed using the Shapiro-Wilk-test. No statistical method was

431   used to calculate sample size, but sample size was determined based on preliminary

432   experiments and previous publications. Analysis was carried out using unpaired Student's *t*-test,

433   Mann-Whitney U test or two-way ANOVA based on data distribution and as indicated. All p-

434   values are two-tailed, and values less than 0.05 were considered statistically significant.

435   GraphPad Prism 8 was used for statistical analysis.

Acknowledgements

We thank Dr. Robin Davisson for guidance on establishing radiotelemetric blood pressure monitoring, Michael N. Singer and Chester Poon for expert IT support and data extraction, Rebecca Teng for assistance in accessing data, and Dr. Barry S. Coller, Dr. Andrew J. Dannenberg, Dr. Javid J. Moslehi and Melissa D. Curtis for valuable discussions during the preparation of this manuscript.

Author Contributions

P.C. and T.B. designed and conceived the study. T.B., D.J.K, S.J.M., A.G.W., I.D.G., S.D.B. and H.S. acquired data and performed experiments. P.C., T.B., S.P., R.V., C.S.J., A.M. and A.D.L. analyzed and interpreted the data. T.B, D.J.K. and P.C. wrote the manuscript with input from all authors.

Competing Interest Statement

All authors declare no competing interests.

Data Availability

Source data for figures 1, 2, 3 as well as extended data figure 1, 2, 4 and 5 are provided with the paper. All other data that support the findings of this study are available from the corresponding author upon reasonable request.

Source of Funding

471

References

1. Rosen, E.D. & Spiegelman, B.M. What we talk about when we talk about fat. *Cell* **156**, 20-44 (2014).

2. Bartelt, A.*, et al.* Brown adipose tissue activity controls triglyceride clearance. *Nat. Med.* **17**, 200-205 (2011).

3. Lowell, B.B.*, et al.* Development of obesity in transgenic mice after genetic ablation of brown adipose tissue. *Nature* **366**, 740-742 (1993).

4. Cohen, P. & Spiegelman, B.M. Brown and Beige Fat: Molecular Parts of a Thermogenic Machine. *Diabetes* **64**, 2346-2351 (2015).

5. Yeung, H.W.*, et al.* Patterns of (18)F-FDG uptake in adipose tissue and muscle: a potential source of false-positives for PET. *J. Nucl. Med.* **44**, 1789-1796 (2003).

6. Cohade, C., Osman, M., Pannu, H.K. & Wahl, R.L. Uptake in supraclavicular area fat ("USA-Fat"): description on 18F-FDG PET/CT. *J. Nucl. Med.* **44**, 170-176 (2003).

7. van Marken Lichtenbelt, W.D.*, et al.* Cold-activated brown adipose tissue in healthy men. *N. Engl. J. Med.* **360**, 1500-1508 (2009).

8. Virtanen, K.A.*, et al.* Functional brown adipose tissue in healthy adults. *N. Engl. J. Med.* **360**, 1518-1525 (2009).

9. Cypess, A.M.*, et al.* Identification and importance of brown adipose tissue in adult humans. *N. Engl. J. Med.* **360**, 1509-1517 (2009).

10. Cronin, C.G.*, et al.* Brown fat at PET/CT: correlation with patient characteristics. *Radiology* **263**, 836-842 (2012).

11. Steinberg, J.D., Vogel, W. & Vegt, E. Factors influencing brown fat activation in FDG PET/CT: a retrospective analysis of 15,000+ cases. *Br. J. Radiol.* **90**, 20170093 (2017).

12. Brendle, C.*, et al.* Correlation of Brown Adipose Tissue with Other Body Fat Compartments and Patient Characteristics: A Retrospective Analysis in a Large Patient Cohort Using PET/CT. *Acad. Radiol.* **25**, 102-110 (2018).

498 13. Ouellet, V*., et al.* Brown adipose tissue oxidative metabolism contributes to energy

499   expenditure during acute cold exposure in humans. *J. Clin. Invest.* **122**, 545-552 (2012).

500 14. Yoneshiro, T*., et al.* Brown adipose tissue, whole-body energy expenditure, and

501   thermogenesis in healthy adult men. *Obesity (Silver Spring)* **19**, 13-16 (2011).

502 15. Orava, J*., et al.* Different metabolic responses of human brown adipose tissue to

503   activation by cold and insulin. *Cell Metab.* **14**, 272-279 (2011).

504 16. Cohade, C., Mourtzikos, K.A. & Wahl, R.L. "USA-Fat": prevalence is related to ambient

505   outdoor temperature-evaluation with 18F-FDG PET/CT. *J. Nucl. Med.* **44**, 1267-1270

506   (2003).

507 17. Kir, S. & Spiegelman, B.M. Cachexia & Brown Fat: A Burning Issue in Cancer. *Trends in*

508   *cancer* **2**, 461-463 (2016).

509 18. Cao, Q*., et al.* A pilot study of FDG PET/CT detects a link between brown adipose tissue

510   and breast cancer. *BMC Cancer* **14**, 126 (2014).

511 19. Fujii, T*., et al.* Implication of atypical supraclavicular F18-fluorodeoxyglucose uptake in

512   patients with breast cancer: Association between brown adipose tissue and breast

513   cancer. *Oncology letters* **14**, 7025-7030 (2017).

514 20. Villarroya, F., Cereijo, R., Villarroya, J. & Giralt, M. Brown adipose tissue as a secretory

515   organ. *Nat Rev Endocrinol* **13**, 26-35 (2017).

516 21. Choi, C.H.J. & Cohen, P. Adipose crosstalk with other cell types in health and disease.

517   *Exp. Cell Res.* **360**, 6-11 (2017).

518 22. Wang, G.X., Zhao, X.Y. & Lin, J.D. The brown fat secretome: metabolic functions

519   beyond thermogenesis. *Trends Endocrinol Metab* **26**, 231-237 (2015).

520 23. Shinoda, K*., et al.* Genetic and functional characterization of clonally derived adult

521   human brown adipocytes. *Nat. Med.* **21**, 389-394 (2015).

522 24. Cohen, P*., et al.* Ablation of PRDM16 and beige adipose causes metabolic dysfunction

523   and a subcutaneous to visceral fat switch. *Cell* **156**, 304-316 (2014).

25. Liu, C., *et al.* Meta-analysis identifies common and rare variants influencing blood pressure and overlapping with metabolic trait loci. *Nat. Genet.* **48**, 1162-1170 (2016).

26. Ward, Z.J., *et al.* Projected U.S. State-Level Prevalence of Adult Obesity and Severe Obesity. *N. Engl. J. Med.* **381**, 2440-2450 (2019).

27. Cypess, A.M. & Kahn, C.R. Brown fat as a therapy for obesity and diabetes. *Curr Opin Endocrinol Diabetes Obes* **17**, 143-149 (2010).

28. Blondin, D.P., *et al.* Dietary fatty acid metabolism of brown adipose tissue in cold-acclimated men. *Nat Commun* **8**, 14146 (2017).

29. Chondronikola, M., *et al.* Brown Adipose Tissue Activation Is Linked to Distinct Systemic Effects on Lipid Metabolism in Humans. *Cell Metab.* **23**, 1200-1206 (2016).

30. Yoneshiro, T., *et al.* Recruited brown adipose tissue as an antiobesity agent in humans. *J. Clin. Invest.* **123**, 3404-3408 (2013).

31. Hanssen, M.J., *et al.* Short-term cold acclimation improves insulin sensitivity in patients with type 2 diabetes mellitus. *Nat. Med.* **21**, 863-865 (2015).

32. Liu, X., *et al.* Brown adipose tissue transplantation improves whole-body energy metabolism. *Cell Res.* **23**, 851-854 (2013).

33. Feldmann, H.M., Golozoubova, V., Cannon, B. & Nedergaard, J. UCP1 ablation induces obesity and abolishes diet-induced thermogenesis in mice exempt from thermal stress by living at thermoneutrality. *Cell Metab.* **9**, 203-209 (2009).

34. Alcala, M., *et al.* Mechanisms of Impaired Brown Adipose Tissue Recruitment in Obesity. *Front Physiol* **10**, 94 (2019).

35. Langenberg, C. & Lotta, L.A. Genomic insights into the causes of type 2 diabetes. *Lancet* **391**, 2463-2474 (2018).

36. Yarnell, J.W., *et al.* Fibrinogen, viscosity, and white blood cell count are major risk factors for ischemic heart disease. The Caerphilly and Speedwell collaborative heart disease studies. *Circulation* **83**, 836-844 (1991).

550   37.   Friedman, G.D., Klatsky, A.L. & Siegelaub, A.B. The leukocyte count as a predictor of

551   myocardial infarction. *N. Engl. J. Med.* **290**, 1275-1278 (1974).

552   38.   Ensrud, K. & Grimm, R.H., Jr. The white blood cell count and risk for coronary heart

553   disease. *Am. Heart J.* **124**, 207-213 (1992).

554   39.   von Elm, E*., et al.* The Strengthening the Reporting of Observational Studies in

555   Epidemiology (STROBE) statement: guidelines for reporting observational studies.

556   *Lancet* **370**, 1453-1457 (2007).

557   40.   McGavigan, A.K*., et al.* Vertical sleeve gastrectomy reduces blood pressure and

558   hypothalamic endoplasmic reticulum stress in mice. *Disease models & mechanisms* **10**,

559   235-243 (2017).

560   41.   Cantalupo, A*., et al.* Nogo-B regulates endothelial sphingolipid homeostasis to control

561   vascular function and blood pressure. *Nat. Med.* **21**, 1028-1037 (2015).

562

563

564

Fig. 1: a, ^{18}F-FDG PET/CT reports were reviewed for reporting of brown adipose tissue between June 2009 and March 2018 and individuals were stratified by presence or absence of brown fat. An index scan was assigned and diagnosis codes and available laboratory values in temporal vicinity were collected. **b,** Brown fat was reported in 5.7% of all ^{18}F-FDG PET/CT scans (n=139,224). **c,** Brown fat was reported in 9.5% of all patients (n=53,475). **d,** Prevalence of brown fat was higher in females compared with males. Groups were compared by chi-square test, *P*-value is two-tailed. **e,** Brown fat prevalence was inversely correlated with age and followed a one-phase decay. Spearman's rank correlation coefficient was calculated to assess the correlation between brown fat prevalence and age, *P*-value is two-tailed. **f,** Brown fat prevalence, based on ^{18}F-FDG PET/CT scans was inversely correlated with outdoor temperature in the month of the scan between June 2009 and March 2018. Bars depict means, error bars are s.e.m., dots are mean temperature for each year between 2009 and 2018. **g,** Brown fat prevalence was inversely correlated with body mass index. **h,** Propensity score matching was used to identify a matched cohort based on age, sex, body mass index and outdoor temperature in the month of the index scan.

580

Fig. 2: a, Comparison of cardiometabolic disease prevalence between individuals with and without brown adipose tissue (BAT). Groups were compared by chi-square test, all *P*-values are two-sided. **b,** Forrest plots illustrate the association between brown fat status and cardiometabolic disease in the propensity score matched cohort. Circles and bars represent odds ratios (ORs) and 95% confidence intervals (CIs), respectively, and were calculated using multivariable logistic regression analysis with adjustment for age, sex, body mass index, outdoor temperature in the month of the index scan, ethnicity, race, smoking status, family history of cardiovascular disease, beta blocker use, cancer site and cancer stage. All *P*-values are two

589   sided. Black circles and CI bars represent non-significant associations, red circles and CI bars

590   represent statistically significant associations at $P < 0.05$. **c**, Prevalence of cardiometabolic

591   disease stratified by brown status and body mass index using the WHO categories for normal

592   and underweight (body mass index (BMI) < 25.0 kg/m^2), overweight (BMI between 25.0 and

593   30.0 kg/m^2) and obesity (BMI > 30.0 kg/m^2). Patients per category: BMI < 25.0 kg/m^2, with

594   brown fat n = 2,564, without brown fat n = 2,639; BMI between 25.0 and 30.0 kg/m^2, with brown

595   fat n = 1,589, without brown fat n = 1,491; BMI > 30.0 kg/m^2, with brown fat n = 917, without

596   brown fat n = 940. Significance was assessed using multivariable logistic regression adjusted

597   for age, sex, body mass index, outdoor temperature in the month of the index scan, ethnicity,

598   race, smoking status, family history of cardiovascular disease, beta blocker use, cancer site and

599   cancer stage. P values are depicted for values <0.1. All P values are two sided. **d**, Comparison

600   of available laboratory values between matched individuals with and brown fat (glucose; with

601   brown fat n = 5,033 (99.3%), without brown fat n = 4,963 (97.9%); triglycerides; with brown fat n

602   = 732 (14.4%), without brown fat n = 734 (14.5%); high-density lipoprotein; with brown fat n =

603   596 (11.8%), without brown fat n= 578 (11.4%); low density lipoprotein; with brown fat n = 543

604   (10.7%), without brown fat n = 527 (10.4%); total cholesterol; with brown fat n = 637 (12.6%),

605   without brown fat n = 630 (12.4%). Groups were compared with Student's t-test, dots represent

606   means, error bars 95% confidence intervals, all P-values are two-sided. Values with statistically

607   significant differences were stratified by body mass index and a linear regression line for body

608   mass index values between 18.5 and 40.0 kg/m^2 was calculated. Shaded areas depict 95%

609   confidence intervals.

610

611   **Fig. 3: a,** Implanted radiotelemetery devices were used to measure systolic, diastolic and mean

612   arterial blood pressure and heart rate in freely moving mice with an adipocyte-specific knockout

613   (KO) of *Prdm16* or wildtype (WT) controls (n=35 per group from a total of 4 independent

614　experiments). Dots depict mean, error bars are s.e.m. A linear mixed model for repeated

615　measures over time was used to analyze the radiotelemetry data with fixed effects of genotype

616　(KO vs. WT), week treated as a categorical factor, and the interaction between genotype and

617　week. [a] denotes *P*-values that were calculated by adjusting the above mentioned linear mixed

618　model by heart rate to account for the observed differences in heart rate. All *P*-values are two-

619　sided. **b**, Heart weight at necropsy normalized to body weight, ejection fraction and fractional

620　shortening (both assessed by echocardiography) were measured in KO (n=12) and WT (n=8)

621　animals. Bars represent means, error bars are s.d. Groups were compared by Student's t-test.

622　All *P*-values are two-sided. **c** Pressure myography after removal of perivascular fat was

623　conducted in KO and WT animals (n=3 per group; 2 mesenteric arteries per mouse) to assess

624　response to acetylcholine (endothelium-dependent vasorelaxation), phenylephrine and

625　angiotensin II (both vasoconstrictions). Dots represent means, error bars are s.e.m. Groups

626　were compared by two-way analysis of variance (ANOVA). All *P*-values are two-sided. **d**,

627　Mesenteric arteries were stained with Masson's trichrome stain to compare WT and KO

628　animals. Representative image, n=5 per group. Scale bar is 50 µm. **e**, Angiotensinogen levels

629　were measured in KO and WT animals using mass spectrometry (n = 8 per group). Groups

630　were compared using Student's t-test. All *P*-values are two-sided. **f**, Expression of angiotensin

631　receptors on mesenteric arteries was assessed using quantitative PCR (qPCR); n=5 per group.

632　Groups were compared using Student's t-test. All *P*-values are two-sided.

633

634　**Extended Data Fig. 1: a**, The total number of ^{18}F-FDG PET/CT scans performed at MSKCC

635　increased from 2009 to 2018 while the prevalence of reported brown fat remained stable. Dots

636　depict total number of ^{18}F-FDG PET/CT scan in each year, half filled dots illustrate years with

637　incomplete reporting. Bars represent prevalence of ^{18}F-FDG PET/CT scans with reported brown

638　fat.

28

639

640   **Extended Data Fig. 2. a,** Correlation between body mass index and prevalence of brown fat

641   reported on ^{18}F-FDG PET/CT. The dotted line depicts a one-phase decay curve, *P*-value was

642   calculated for the correlation between both variables using Spearman's r. **b**, Correlation

643   between outside temperature in the month of the scan and prevalence of brown fat reported on

644   ^{18}F-FDG PET/CT. The dotted line depicts a linear regression line, *P*-value was calculated for the

645   correlation between both variables using Spearman's r. All *P*-values are two-sided.

646

647   **Extended Data Fig. 3.** Propensity score matching was assessed by comparing standardized

648   mean differences before and after the matching process. The blue shaded area indicates the

649   chosen caliper width.

650

651   **Extended Data Fig. 4. a**, The loxP sites flanking exon 9 and the adiponectin driven Cre-

652   recombinase that were used to create the *Prdm16* knockout (KO) mouse model are shown.

653   Radio telemetry devices to measure blood pressure were implanted in mice between the age of

654   11 and 14 weeks and measurements were started 1 week after implantation for 3 weeks.

655   Pressure myography and echocardiography were performed at the end of the study. **b**,

656   Expression of *Prdm16* in brown adipose tissue (BAT), subcutaneous adipose tissue (SQ) and

657   visceral adipose tissue (Visc) was measured by quantitative PCR (qPCR) and compared

658   between KO (n=8) and littermate control wildtype animals (WT; n=8). Groups were compared

659   using Mann-Whitney U test for non-normally distributed variables (BAT) and Student's t-test for

660   normally distributed variables (SQ and Visc). Bar depict means, error bars are s.e.m. All *P*-

661   values are two-sided. **c**, Expression of *Prdm16* in mesenteric arteries and adjacent mesenteric

662   adipose tissue was measured by quantitative PCR (qPCR) and compared between KO (n=4 for

663   mesenteric arteries' n=5 for mesenteric fat) and littermate control wildtype animals (WT; n=4 for

664   mesenteric arteries' n=5 for mesenteric fat). Groups were compared using Student's t-test. Bar

665   depict means, error bars are s.e.m. All *P*-values are two-sided. **d**, Comparison of body weights

666   between WT and KO animals (both n=35 at the beginning of the study). Groups were compared

667   using a mixed effects model with post-hoc analysis for individual time points.

668

669   **Extended Data Fig. 5. a**, Sections of the left ventricle were stained with Masson's trichrome

670   stain to compare fat specific *Prdm16* knockout (KO) and littermate control (wildtype; WT)

671   animals. Representative image, n=5 per group. Scale bar is 50 µm. **b**, Mesenteric arteries from

672   KO and WT were harvested, cleaned of perivascular fat and used for pressure myography (n=3

673   per group). Groups were compared using two-way analysis of variance (ANOVA). Dots

674   represent means, error bars s.e.m. All *P*-values are two-sided.

675

Table 1. Characteristics of Patients with and without Brown Fat Before and After Propensity Score Matching

Baseline Variable	Before Propensity Score Matching		After Propensity Score Matching		P-Value[*]
	Brown Adipose Present (BAT+) (N=5 070)	Brown Adipose Absent (BAT-) (N=48 405)	Brown Adipose Present (BAT+) After Matching (N=5 070)	Brown Adipose Absent (BAT-) After Matching (N=5 070)	
Age, mean (SD)	49.0 (16.3)	61.7 (14.0)	49.0 (16.3)	49.2 (15.8)	0.5863
Sex, No. (%)					
Women	3 879 (76.5)	24 711 (51.1)	3 879 (76.5)	3 879 (76.5)	1.0000
Men	1 191 (23.5)	23 694 (49.0)	1 191 (23.5)	1 191 (23.5)	
BMI, mean (SD)	25.8 (5.3)	27.8 (5.9)	25.8 (5.3)	25.6 (5.5)	0.0830
BMI category, No. (%)					
< 25.0	2,564 (50.6)	16,578 (34.3)	2,564 (50.6)	2,639 (52.1)	<0.0001
25.0 – 29.9	1,589 (31.3)	17,436 (36.0)	1,589 (31.3)	1,491 (29.4)	
> 30.0	917 (18.1)	14,391 (29.7)	917 (18.1)	940 (18.5)	
Race, No. (%)					
Asian	402 (7.9)	2 851 (5.9)	402 (7.9)	414 (8.2)	<0.0001
African American	561 (11.1)	3 396 (7.0)	561 (11.1)	434 (8.6)	
Caucasian	3 694 (72.9)	39 225 (81.0)	3 694 (72.9)	3 862 (76.2)	
Other or Unknown	413 (8.2)	2 933 (6.1)	413 (8.2)	360 (7.1)	
Ethnicity, No. (%)					
Hispanic	398 (7.9)	2 803 (5.8)	398 (7.9)	330 (6.5)	0.0281
Non-Hispanic	4 458 (87.9)	43 059 (89.0)	4 458 (87.9)	4 534 (89.4)	
Unknown	214 (4.2)	2 543 (5.3)	214 (4.2)	206 (4.1)	
Cardiovascular Risk Factors, No. (%)					
Family History of Cardiovascular Disease	1 029 (20.3)	11 714 (24.2)	1 029 (20.3)	1 086 (21.4)	0.1636
Smoking Status					
Current Smoker	513 (10.1)	5 390 (11.1)	513 (10.1)	588 (11.6)	<0.0001
Previous Smoker	1 169 (23.1)	17 755 (36.7)	1 169 (23.1)	1 261 (24.9)	
Never Smoker	2 999 (59.2)	19 923 (41.2)	2 999 (59.2)	2 654 (52.4)	
Unknown	389 (7.7)	5 337 (11.0)	389 (7.7)	567 (11.2)	
^{18}F-FDG PET/CT Characteristics					
Total Number of Scans per Patient, n (%)	4.1 (4.0)	2.5 (2.6)	4.1 (4.0)	2.5 (3.8)	<0.0001
Temperature (°C Month of Reference Scan), mean (SD)	11.9 (8.6)	13.6 (8.8)	11.9 (8.6)	12.0 (8.8)	0.7242
Beta blocker, n (%)	656 (12.9)	12 569 (26.0)	656 (12.9)	899 (17.7)	<0.0001

*P-value for the comparison of BAT+ and BAT- individuals in the propensity score matched group.

BAT, brown adipose tissue. SD, standard deviation. BMI, body mass index.

676

Fig. 1: Identification of brown fat and association with age, sex, body mass index and outdoor temperature. A propensity score matched cohort was constructed to adjust for differences in these individuals.

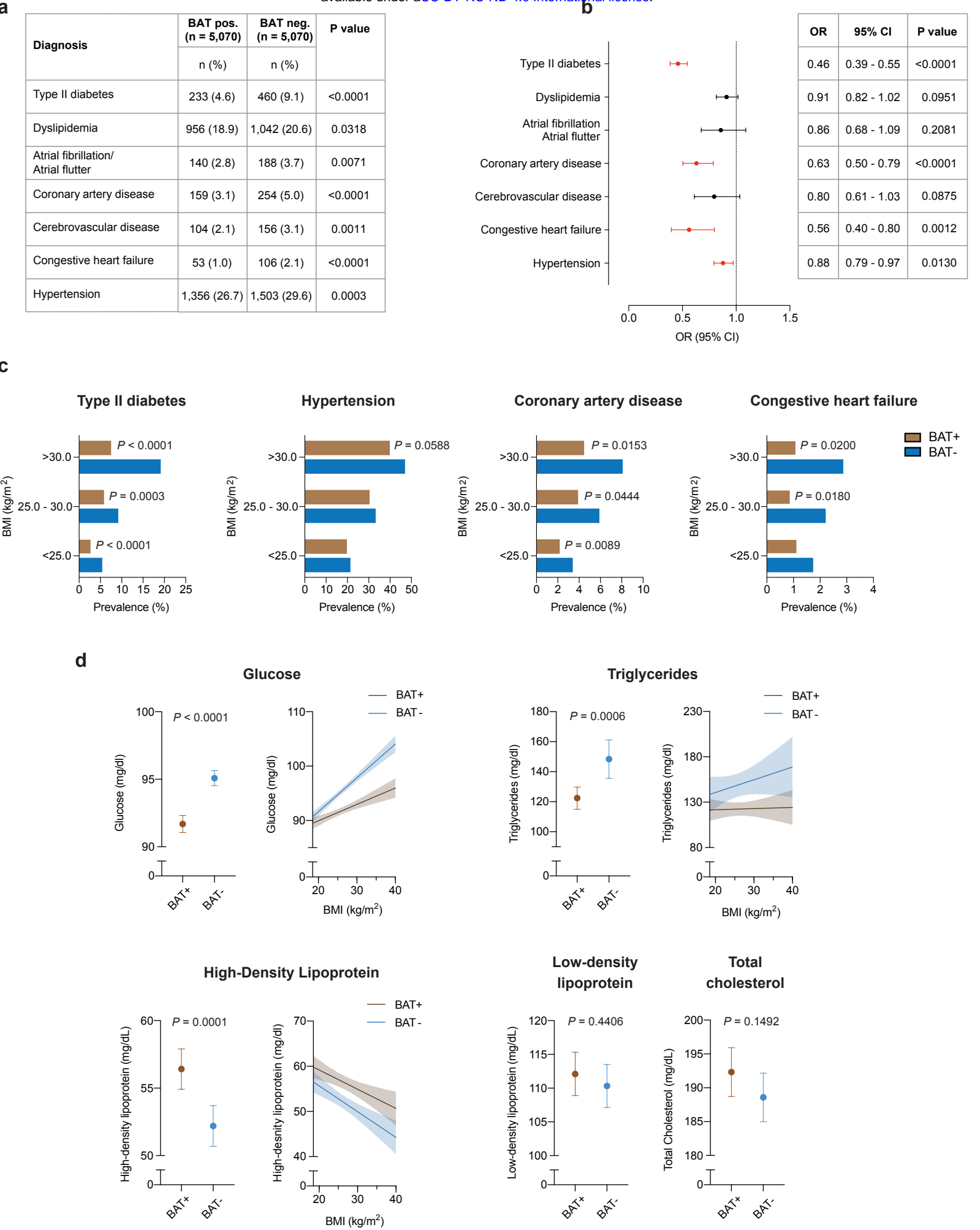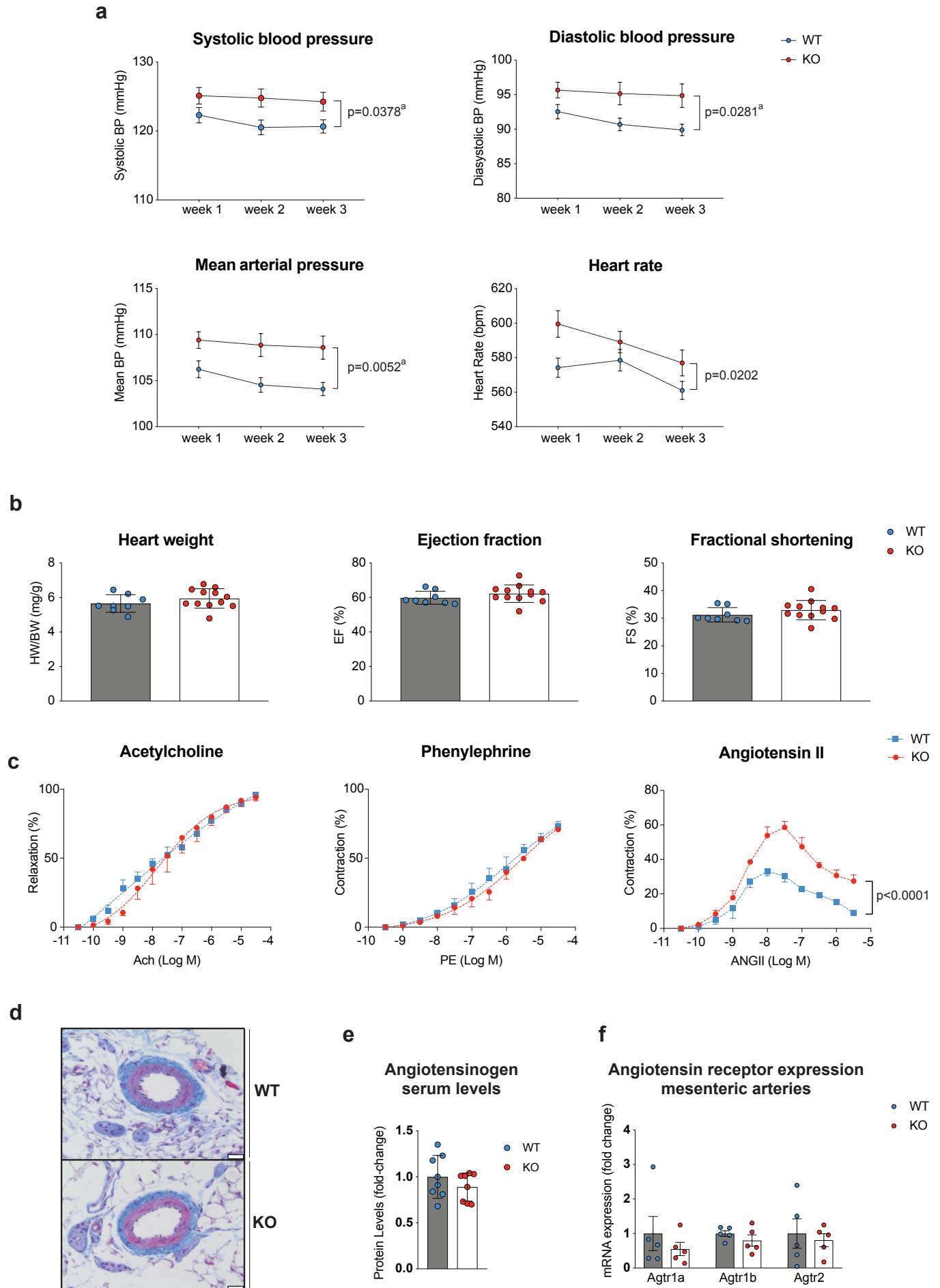**Fig. 2: Brown fat is associated with improved cardiometabolic health.**

a

Diagnosis	BAT pos. (n = 5,070)	BAT neg. (n = 5,070)	P value
	n (%)	n (%)	
Type II diabetes	233 (4.6)	460 (9.1)	<0.0001
Dyslipidemia	956 (18.9)	1,042 (20.6)	0.0318
Atrial fibrillation/ Atrial flutter	140 (2.8)	188 (3.7)	0.0071
Coronary artery disease	159 (3.1)	254 (5.0)	<0.0001
Cerebrovascular disease	104 (2.1)	156 (3.1)	0.0011
Congestive heart failure	53 (1.0)	106 (2.1)	<0.0001
Hypertension	1,356 (26.7)	1,503 (29.6)	0.0003

b

	OR	95% CI	P value
Type II diabetes	0.46	0.39 - 0.55	<0.0001
Dyslipidemia	0.91	0.82 - 1.02	0.0951
Atrial fibrillation Atrial flutter	0.86	0.68 - 1.09	0.2081
Coronary artery disease	0.63	0.50 - 0.79	<0.0001
Cerebrovascular disease	0.80	0.61 - 1.03	0.0875
Congestive heart failure	0.56	0.40 - 0.80	0.0012
Hypertension	0.88	0.79 - 0.97	0.0130

c

d

Fig 3. Ablation of thermogenic fat induces hypertension

Extended Data Fig. 1: Number of ^{18}F-FDG PET/CT scans and brown fat prevalence between 06/2009 - 03/2018.
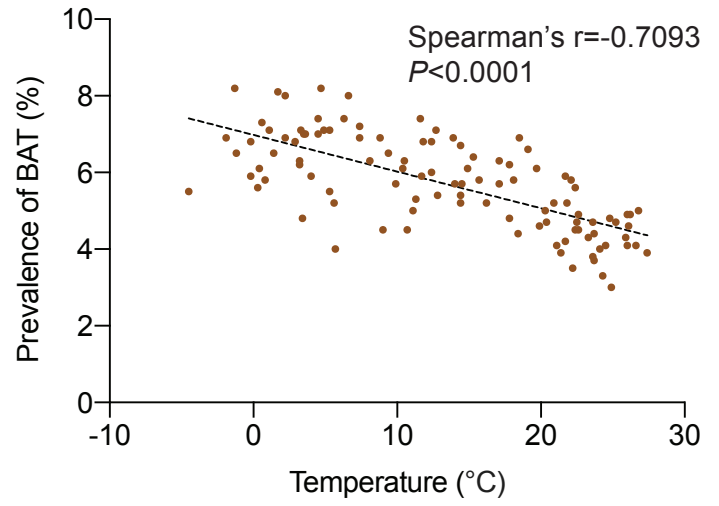
a

b
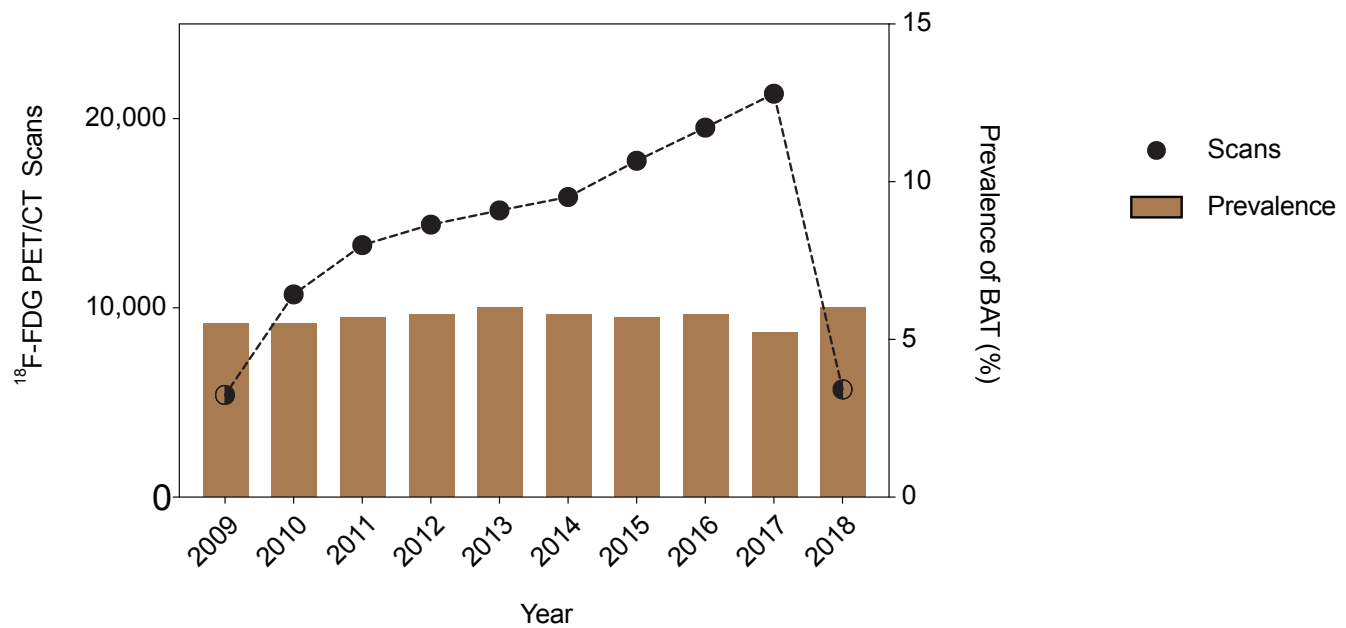
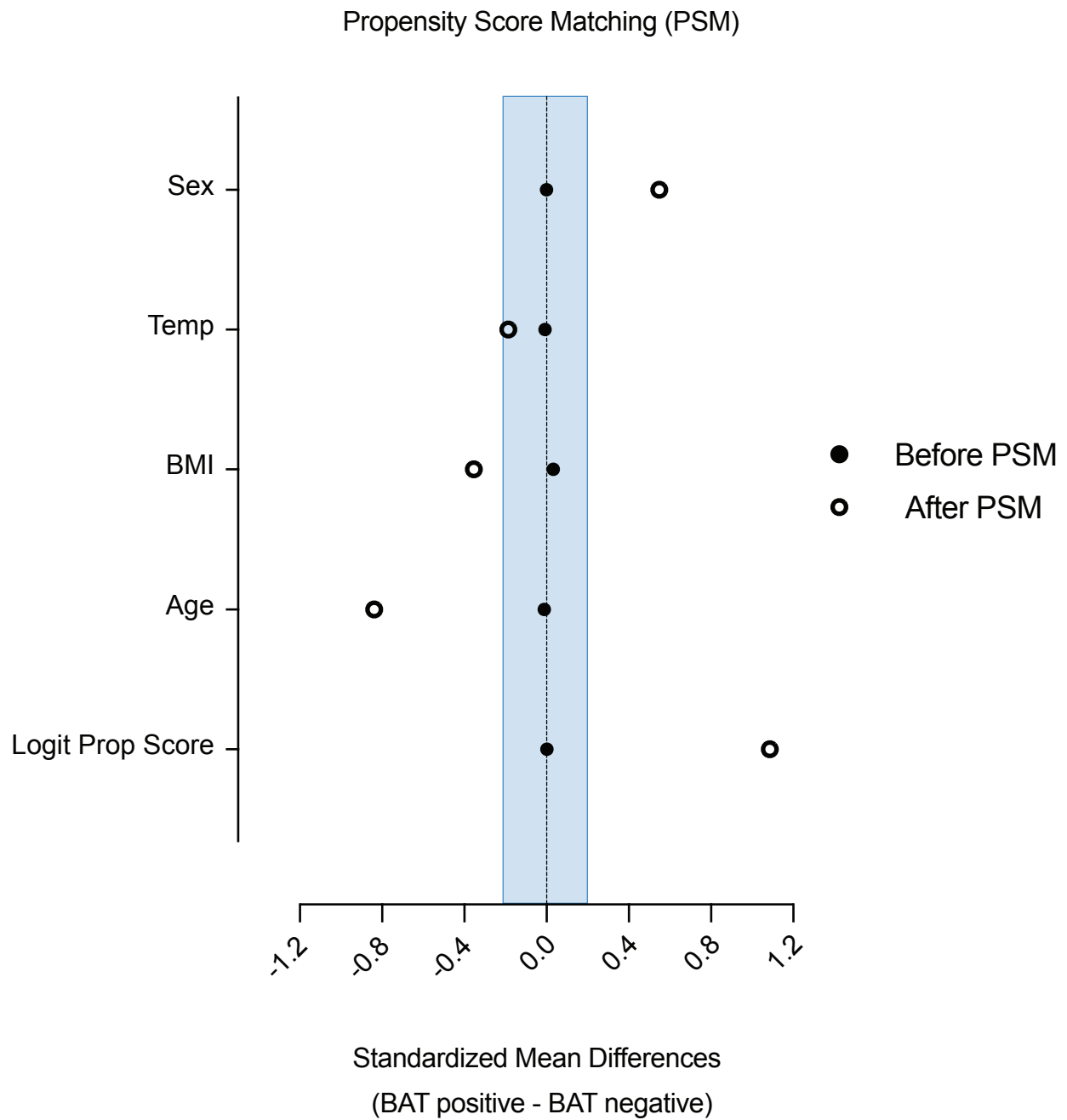**Extended Data Fig. 2: Correlation between brown fat prevalence and body mass index or outside temperature.**
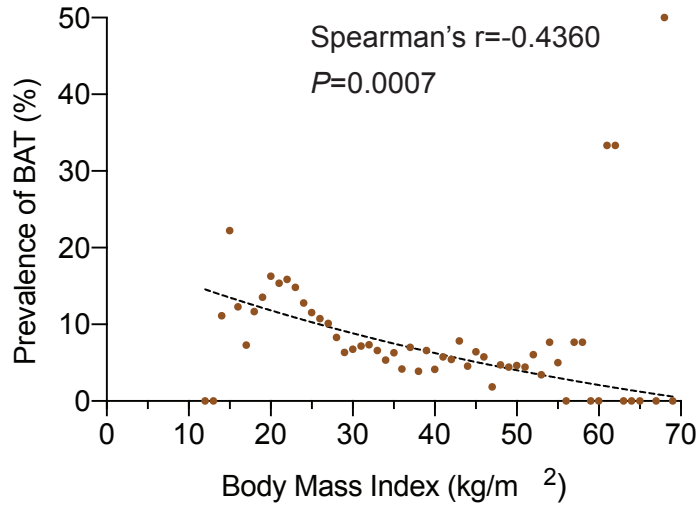
Extended Data Fig. 3: Standardized mean differences before and after propensity score matching.
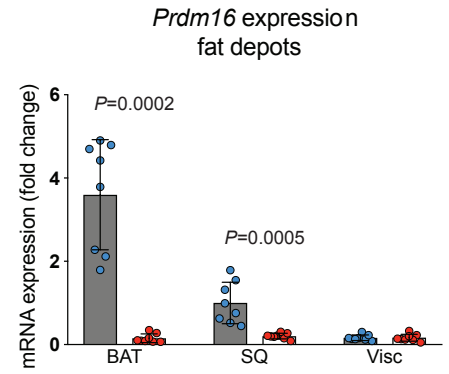

Propensity Score Matching (PSM)

Standardized Mean Differences

(BAT positive - BAT negative)

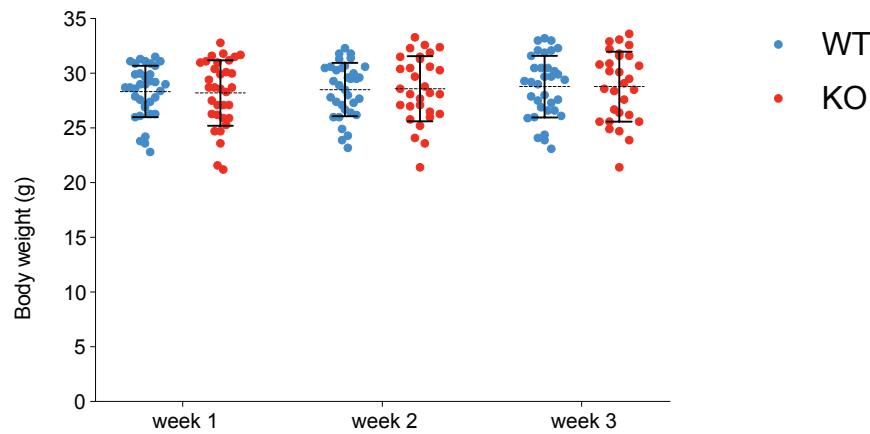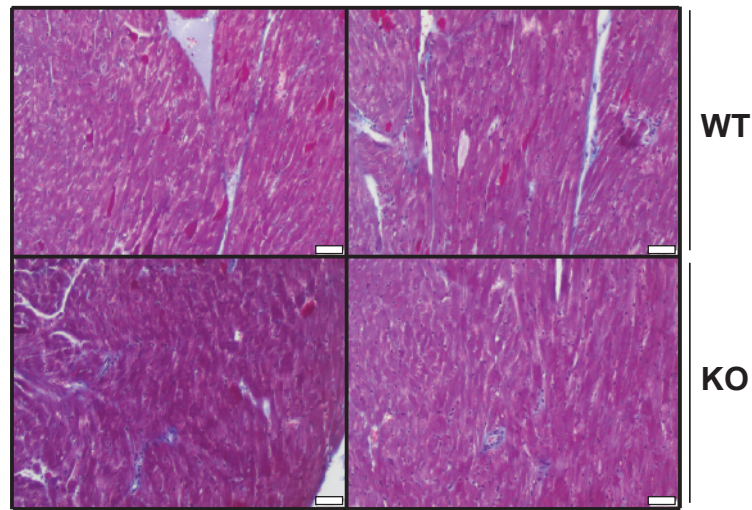**Extended Data Fig. 4: Study design and characteristics of the prdm16 mouse model.**
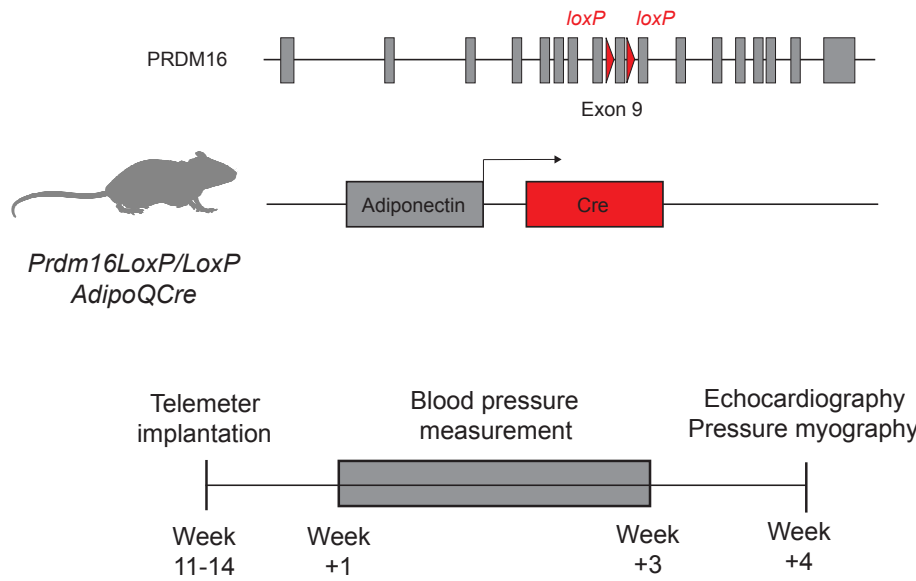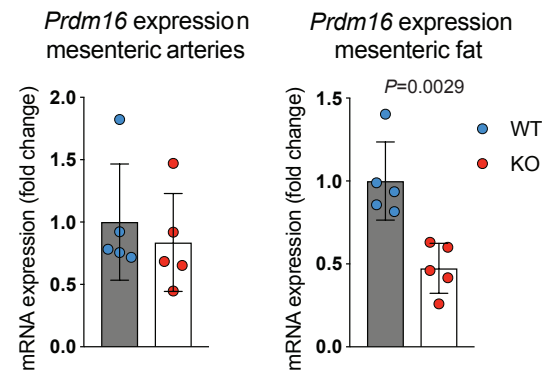
Extended Data Fig. 5: Cardiac histology and pressure myography.

a

b